JOURNAL OF APPLIED ELECTROCHEMISTRY 20 (1990) 447–453

The relationship between the growth rate of hydrogen bubbles and the duration of the 'induction period' in the electrowinning of zinc from sulphate electrolytes

CHR. BOZHKOV, I. IVANOV, ST. RASHKOV

Bulgarian Academy of Sciences, Institute of Physical Chemistry, Sofia 1040, Bulgaria

Received 26 June 1989, revised 18 August 1989

As a result of detailed polarization, volumetric and optical *in situ* investigations of the growth rate of hydrogen bubbles during the electrowinning of zinc from Ni^{2+}-containing sulphate electrolytes and in the presence of an inhibitor, a relationship has been established between the shape of the hydrogen bubbles and the duration of the 'induction period'. It has been found that during the 'induction period' hydrogen bubbles alter their shape from spherical at the beginning to cupola-shaped at the end, thus increasing by 10–12 times the extent of the screening of the cathode surface beneath. Experimental confirmation is presented for the validity of the previously proposed [1] physical model for the nature of the 'induction period'.

1. Introduction

As a result of detailed electron microscopic, voltammetric and optical *in situ* studies reported in a previous paper [1], it was shown that during the electroextraction of zinc from Ni^{2+}-containing sulphate electrolytes a certain relationship exists between the duration of the induction period and the wetting angle (θ) of the hydrogen bubbles growing on the electrode surface. On the basis of these investigations a physical model was proposed offering an explanation of the nature of the induction period. This model is based on the screening effect with respect to the cathodic current consequent on growing hydrogen bubbles at definite sites on the electrode surface enriched by codeposited nickel.

This approach [1] offers a reasonable prediction of the duration of the 'induction period' with variation of some technologically important parameters in the electrowinning process; temperature, pH, chemical composition of the substrate of the electrode, cathode potential, presence of surfactants, and so on.

This paper is an attempt to check experimentally the assumptions of the model with respect to the effect of some surfactants which have a well established influence on supressing the negative action of impurities such as Ni^{2+}.

On the other hand, as mentioned in [1], the mean attachment time, $\bar{\tau}_1$ of the hydrogen bubbles before being detached from the electrode surface is within the order of 5–15 min, a period considerably shorter than the duration, t, of the induction period.

It has been established [2] that in the presence of 5–10 mg l^{-1} Ni^{2+}-containing solutions, t has a value of 90–150 min. This requires the establishment of an interrelationship between these two periods ($\bar{\tau}_1$ and t) by studying the changes in the shape, average lifetime and growth rate of the hydrogen bubbles during the 'induction period' as well as during the active 'self-dissolution' of zinc.

2. Theoretical

It is well known from the investigations dealing with gas evolution on solid electrodes [3] that the equilibrium state of a gas bubble on the electrode surface is determined by the effects of two forces: capillary (F_c) and hydrostatic (F_h). The former acts along the perimeter of the gas bubble–solid surface contact surface and is equal to the product of this perimeter and the vertical component of the surface tension between the liquid and gas phase:

$$F_c = \pi d\sigma_{23} \sin \theta \quad (1)$$

The value of the wetting angle, θ, is determined by the ratio between the surface tension values among the three phases (solid–liquid–gas) according to Young's equation:

$$\cos \theta = \frac{\sigma_{13} - \sigma_{12}}{\sigma_{23}} \quad (2)$$

where d is the diameter of the gas bubble–surface contact circle, θ is the wetting angle metal–electrolyte–gas and σ_{12}, σ_{13} and σ_{23} are the surface tensions between the phases solid–liquid, solid–gas and liquid–gas, respectively. The hydrostatic force, F_h, can be determined by Archimedes' law:

$$F_h = Vgq \quad (3)$$

Since Equation 3 does not take into account the forces acting on the surface of the gas bubble during its growth, a more accurate and experimentally confirmed equation for F_h has been proposed by Kabanov

0021-891X/90 $03.00 + .12

and Frumkin [4]:

$$F_h = Vgq + \frac{\pi d^2}{4}\left(\frac{2\sigma_{23}}{R} - hg\rho\right) \quad (4)$$

where ϱ is the specific density of the electrolyte, V is the volume of the gas bubble, g is the gravitation constant, h is the height of the gas bubble and R is the radius of the gas bubble at its highest part.

Several studies by Soviet authors [4, 5] have shown that the gas bubble is detached from the electrode surface when the two forces F_c and F_h become equal. This, in turn, presumes the attaining of the critical size by the gas bubble at the moment of its detachment, which can be determined when both forces F_c and F_h become equal:

$$\pi d_{crit}\sigma_{23}\sin\theta_{crit} = V_{crit}g\rho + \frac{\pi d_{crit}^2}{4}\left(\frac{2\sigma_{23}}{R_{crit}} - h_{crit}g\rho\right) \quad (5)$$

These crictical values of the parameters of the detaching bubble can be determined experimentally by accurate photography of the growth process and gas bubble detachment from the electrode surface. The time dependence of the parameters θ_τ, h_τ and d_τ, which are subjected to changes within the period of gas bubble initiation and detachment, can describe the growth kinetics.

On the other hand, an important peculiarity in the case of gas evolution on electrically charged metal surfaces (electrodes) is the relationship between σ_{12}, and the electrode potential, E, or, more precisely, the electrode charge. It has been established that, regardless of the nature of the metal or gas [3, 4], the maximum σ_{12} value is reached at the zero charge potential of the metal, E_{zc} while the other two surface tensions, σ_{13} and σ_{23}, are not dependent on the electrode potential.

Several conclusions may be drawn from the consideration above. First Equations 2 and 5 suggest that every overvoltage, η, with respect to the zero charge potential of the electrode should lead to a decrease of σ_{12} and, as a result, the wetting angle should be less. Consequently, a gas bubble with maximum wetting angle θ will remain attached to the cathode at its zero charge potential, E_{zc}.

Secondly, the absorption of surfactants at the solid–electrolyte interface or electrolyte–gas bubble interface will lead to a decrease in the value of σ_{12} and σ_{23} respectively [6]. As a result the expected effect according to Equations 2 and 5 will be expressed as a decrease of the wetting angle θ.

Thirdly, during the electrolysis process under potentiostatic conditions at constant electrode charge (that is, at a constant σ_{12}), it is possible, by measuring the values of θ, h and d, to obtain experimentally the numerical value σ_{23} by applying

$$\sigma_{23} = \frac{g\varrho(V - \pi d^2 h/4}{\pi d(\sin\theta - d/2R)} \quad (6)$$

In addition σ_{23} can be determined (for the sake of comparison) by routine physicochemical tensiometric techniques [6].

Fourthly all quantities in Equations 1–6 with the exception of σ_{13}, can be determined experimentally by photography of the initiation, growth and detachment of the gas bubbles from the electrode surface.

The experimental confirmation of these assumptions, logically ensuring from the proposed physical model [1], was the objective of this investigation.

3. Experimental details

The experiments were carried out in a constant-temperature three-electrode cell with a volume of 0.5 dm^3, equipped with glass bell and a burette, positioned above the cathode, so as to collect and measure the volume of evolved hydrogen. This offered the possibility of determining volumetrically the current yield of hydrogen (CE_H) during the electrolysis process. The cathodes were aluminium plates (Riedel) with an area of 7.5 cm^2, subjected to preliminary polishing with 400 gauge emery paper. The counter-electrodes were Pb-1% Ag alloy anodes, fixed coaxially with respect to the cathode. The reference was a mercury sulphate electrode.

The base electrolyte contained (in $g\,l^{-1}$): H_2SO_4 130; $ZnSO_4 \cdot 7H_2O$ 220; $MnSO_4 \cdot H_2O$ 15.5. Nickel salt was added to the electrolyte, so that its bulk concentration reached 10 $mg\,l^{-1}$ Ni^{2+}. The inhibitor used was added to the electrolyte at a concentration of 5 $ml\,l^{-1}$. The electrolysis was carried out at a temperature of 37 $\pm$ 1° C and pH 0.2. The process was performed under galvanostatic conditions at a current density of 5 $A\,dm^{-2}$. Experiments under potentiostatic conditions were also performed at a potential of $-1.58\,V_{sse}$.

The process of hydrogen bubble growth and detachment from the electrode surface was investigated *in situ* by photography. A Zeiss optical microscope was used at magnifications of 32, 50 and 100×. The specially designed glass cell was provided with two oppositely fixed plane-parallel glass windows for illumination and photography of the cathode. The design of the cell and the operation mode is described in detail in [1]. The accuracy attained in the measurement of θ was $\pm 5°$.

The measurement of the surface tension on the electrolyte–gas interface was carried out with a digital tensiometer (type K10T-Kruss) with sensitivity 0.1 $dyn\,cm^{-1}$ [7].

4. Results and discussion

The changes in the current yield of hydrogen (CE_H) with time of electrolysis, T, under galvanostatic conditions at $I = 5\,A\,dm^{-2}$ are shown in Fig. 1. Curve 1, in the presence of Ni^{2+}, clearly displays two regions. The first, A, is obtained during the induction period, and the second, B, is obtained during the active 'self-dissolution' of the zinc deposit. The latter, obtained at the end of the induction period (after 2 h of depo-

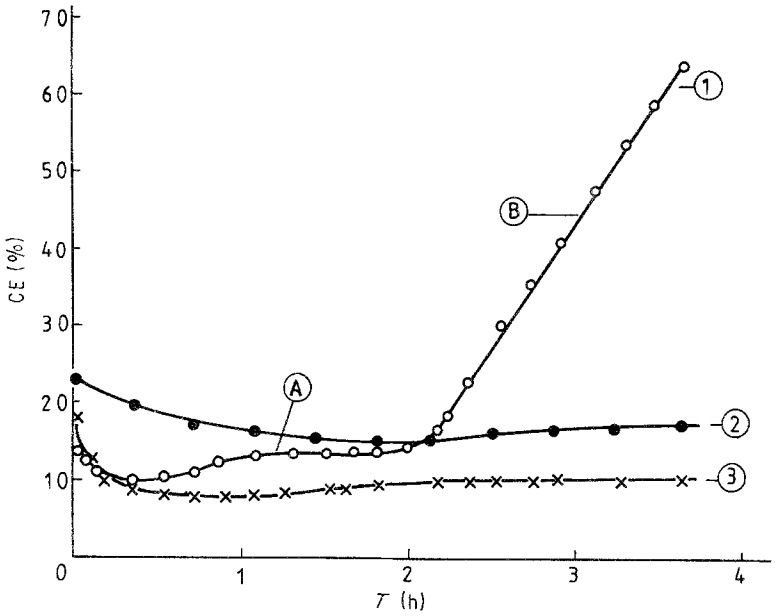

Fig. 1. Time dependence of the current yield of hydrogen, CE_H, established at $I = 5\,A\,dm^{-2}$ in (curve 1) basic electrolyte with $10\,mg\,l^{-1}$ Ni^{2+}, (curve 2) basic electrolyte with $10\,mg\,l^{-1}$ Ni^{2+} and $5\,ml\,l^{-1}$ inhibitor and (curve 3) basic electrolyte.

sition), displays a characteristic morphology (Fig. 2a) with clear-cut pitting defects, reaching a depth down to the aluminium cathode substrate. These basic defects on which the zinc corrosion process is developed correspond to the growth sites of the hydrogen bubbles [1].

The addition of an inhibitor to the nickel-containing electrolyte stabilizes the zinc deposition regime (curve 2 of Fig. 1) and completely eliminates the pitting defects (Fig. 2b). The current yield (CE_H) in the presence of an inhibitor is only 5% higher than the value measured in the Ni-free electrolyte (curve 3 of Fig. 1). The comparison with scanning electron micrographs suggests that in the presence of inhibitor the hydrogen bubbles have a short residence time on the electrode surface, which is not adequate for the creation of pitting defects.

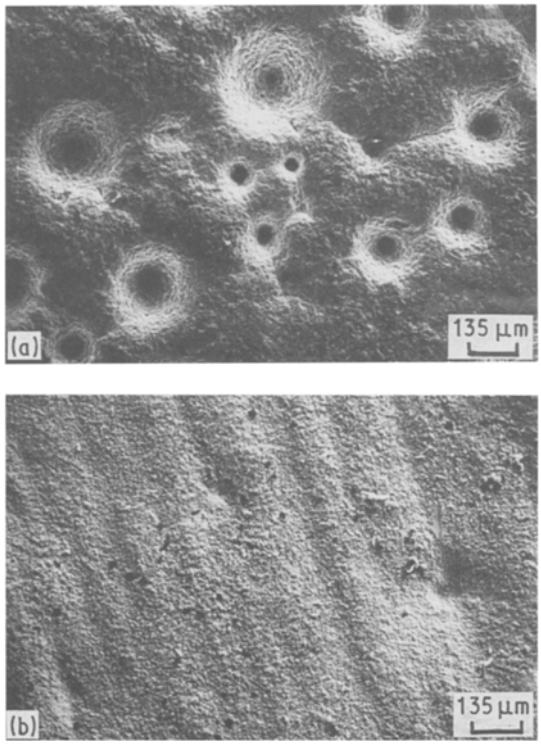

Fig. 2. Scanning electron micrographs of a zinc deposit obtained at $I = 5\,A\,dm^{-2}$ and deposition time $T = 2\,h$, from: (a) basic electrolyte with $10\,mg\,l^{-1}$ Ni^{2+} and (b) basic electrolyte with $10\,mg\,l^{-1}$ Ni^{2+} and $5\,ml\,l^{-1}$ inhibitor.

The common feature of the results presented in Fig. 1 is the fact that higher CE_H values are related to more positive working cathode potentials. Thus, while during the induction period (curve 1, part A), $E \sim -1.58$ V, within the region of the active self-dissolution (curve 1, part B), $E \sim -1.42$ to -1.45 V, the latter potential being almost equal to the corrosion potential of a zinc electrode in this electrolyte. These changes in the cathodic potential, as already mentioned in Section 2, should change the value of σ_{12} and, in agreement with Equation 2, change the wetting angle of the hydrogen bubbles.

The change of the wetting angle, θ, with electrolysis time, T, in the base electrolyte (curve 1) and in the nickel-containing electrolyte (curve 2) is shown in Fig. 3. It is noted that during the induction period θ increases and reaches a maximum value (about 65–70°), then is abruptly reduced to (about 18–20°) within the region of active self-dissolution. A similar wetting angle (20–23°) is maintained during the entire duration of the electrolysis ($T = 6\,h$), both in the basic electrolyte (curve 1) and in the nickel + inhibitor-containing electrolyte (curve 3). Curve 4 shows the change of θ in an electrolyte containing Ni^{2+}, but under potentiostatic electrolysis at $E = -1.58$ V. The comparison between curves shows that the duration of the induction period depends strongly on the value of the cathodic potential since, under potentiostatic conditions, the induction period is twice as long as the case when the electrolysis proceeds under galvanostatic conditions. As was shown in [1] in the presence of $10\,mg\,l^{-1}$ Ni^{2+} the polarization curve, obtained under galvanostatic conditions, gradually, but in a definite way, shifts to more positive potentials as deposition time elapses.

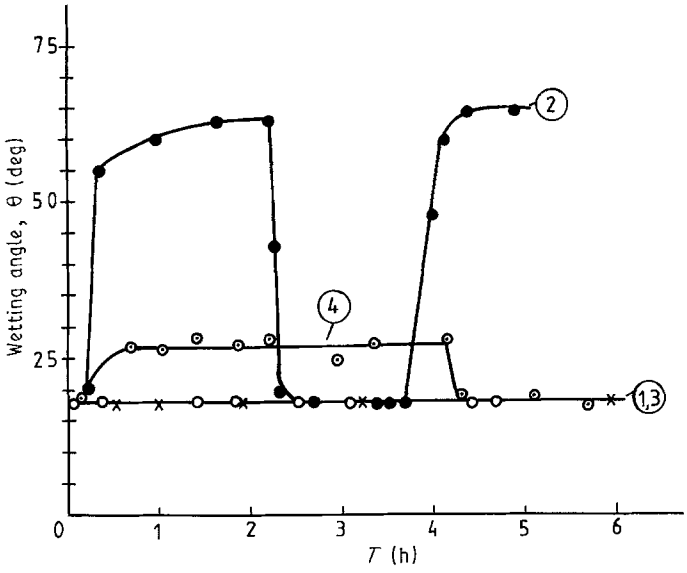

Fig. 3. Time dependence of the mean wetting angle, $\bar{\theta}$, of hydrogen bubbles established in (curve 1) basic electrolyte at $I = 5\,A\,dm^{-2}$, (curve 2) basic electrolyte with $10\,mg\,l^{-1}$ Ni^{2+}, $I = 5\,A\,dm^{-2}$, (curve 3) basic electrolyte with $10\,mg\,l^{-1}$ Ni^{2+} and $5\,ml\,l^{-1}$ inhibitor at $I = 5\,A\,dm^{-2}$ and (curve 4) basic electrolyte with $10\,mg\,l^{-1}$ Ni^{2+} at $E = -1.58\,V_{sse}$.

The effect of the inhibitor is explained by its absorption on the cathode. In this case the electrolysis proceeds at a more negative potential ($E \sim -1.66$ V). Also, tensiometric measurements of the surface tension on the electrolyte–gas interface provide evidence that σ_{23} decreases from $73.2\,dyn\,cm^{-1}$ in the basic electrolyte to about $32.3\,dyn\,cm^{-1}$ in inhibitor-containing electrolytes. The impurity metal (Ni^{2+}) has no effect on σ_{23}. The increased overvoltage, η, and the reduced surface tension, σ_{23}, simultaneously reduce θ, as observed experimentally in Fig. 3, curve 3.

It becomes possible to determine, from continuous photography of the electrode surface, the magnitudes θ_τ, h_τ and d_τ for a separate hydrogen bubble during its growth. The values corresponding to the moment when the bubble is detached from the cathode are denoted as critical values in the text: (θ_{crit}, h_{crit} and d_{crit}), respectively. The change in h_{crit} of hydrogen bubbles is plotted against the duration of electrolysis in Fig. 4. In the case of the base electrolyte (curve 1) and in electrolytes containing nickel with an inhibitor (curve 2) h_{crit} increases gradually with time and reaches 180–200 μm, in the presence of only nickel (curve 3) h_{crit} decreases abruptly from about 250 to about 60 μm during the transition from the induction period to the active 'self-dissolution stage'. The similar character of the changes of h_{crit} (curve 3) with θ (curve 2 of Fig. 3) reflects the pronounced change of the dimensions of the hydrogen bubbles at the end of the induction period.

In this respect it appeared interesting to establish the relationship between the mean attachment time, $\bar{\tau}_1$, of hydrogen bubbles and the duration of electrolysis. These results are presented in Fig. 5. They show that at the end of the induction period in a nickel-containing solution (curve 1) $\bar{\tau}_1$ decreases abruptly from 20–25 min to a few seconds during the zinc 'self-dissolution' process.

The results presented above show that at the end of the induction period (after about 2 h of deposition)

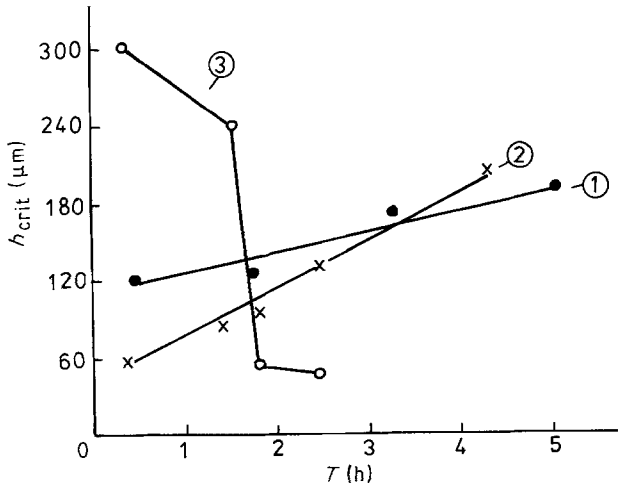

Fig. 4. Time dependence of the critical height, h_{crit}, of the hydrogen bubbles obtained at $I = 5\,A\,dm^{-2}$ in: (curve 1) basic electrolyte, (curve 2) basic electrolyte with $10\,mg\,l^{-1}$ Ni^{2+} and inhibitor $5\,ml\,l^{-1}$ and (curve 3) basic electrolyte with $10\,mg\,l^{-1}$ Ni^{2+}.

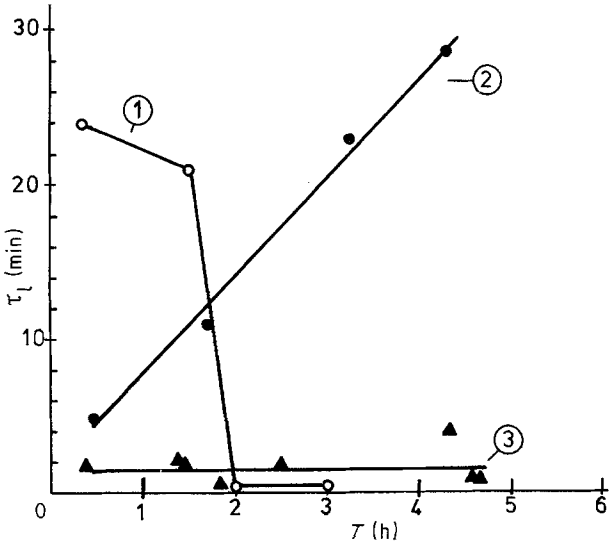

Fig. 5. Time dependence of the mean attachment time, $\bar{\tau}_1$, of the hydrogen bubbles obtained at $I = 5\,A\,dm^{-2}$ in: (curve 1) basic electrolyte with $10\,mg\,l^{-1}$ Ni^{2+}, (curve 2) basic electrolyte and (curve 3) basic electrolyte with $10\,mg\,l^{-1}$ Ni^{2+} and inhibitor $5\,ml\,l^{-1}$.

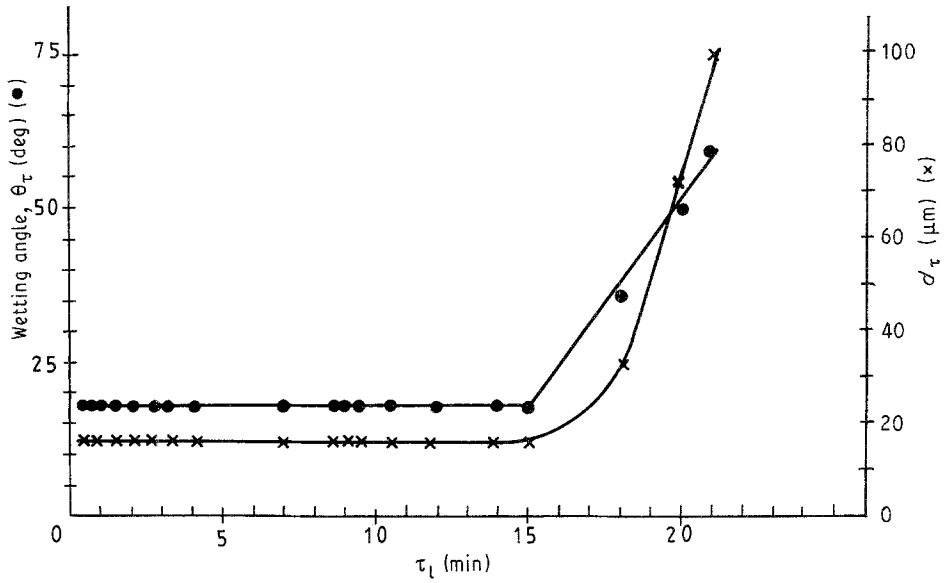

Fig. 6. Time dependence of the parameters θ_τ and d_τ of the hydrogen bubble during its attachment time in the range of the induction period.

hydrogen bubbles have a maximum wetting angle (Fig. 3, curve 2), maximum height (Fig. 4, curve 3) and maximum attachment time (Fig. 5, curve 1), which abruptly decrease during the process of active 'self-dissolution'.

The change in θ_τ and d_τ during the induction period in the presence of nickel is shown in Fig. 6. It is noted that after 15 min these parameters increase abruptly up to about 100 μm for d and about 55–60° for θ. Similar measurements in the base electrolyte and in inhibitor-containing formulations show that hydrogen bubbles have constant values of $\theta \sim 18°$ and $d \sim 6\,\mu$m during their entire attachment time. A similar change of h_τ for a hydrogen bubble in the basic electrolyte (curve 1) and in the presence of nickel (curve 2) during the induction period and in the presence of an inhibitor (curve 3) are shown in Fig. 7. The slopes of these curves provide data for the determination of the growth rate of the height of the bubbles, which is about 6 μm min^{-1} for the base electrolyte, about 12 μm min^{-1} for electrolytes containing Ni^{2+} and about 45 μm min^{-1} for inhibitor-containing electrolytes. Thus, in the latter case the growth rate of hydrogen bubbles is 7–8 times faster, probably due to the specific action of the inhibitor.

The general conclusion, based on the results shown in Figs 6 and 7, suggests that two completely different cases of hydrogen bubble growth are observed. In the first case in the base electrolyte and inhibitor-containing electrolytes, hydrogen bubbles grow only in height, retaining approximately constant wetting angle, θ, and gas bubble–surface contact circle diameter, d. Therefore the bubbles remain approximately spherical during their attachment time (Fig. 8a). In the second case, observed in Ni^{2+}-containing electrolytes, the growing bubbles simultaneously experience a change in both θ and d during the induction period. The initial spherical shape changes to a cupola shape with maximum contact area with the cathode; that is, there is a maximum screening effect of the electrode surface under bubbles (Fig. 8b). This substantial difference has been established on the basis of numerous photographs (Fig. 9).

Consequently, during the induction period, hydrogen bubbles with a mean attachment time longer than 15 min develop a diameter of contact area with the cathode 10–12 times larger than bubbles formed at an identical time in the base electrolyte, or in inhibitor-containing electrolytes. This is obviously a result mainly of the change in θ, which leads to the alteration

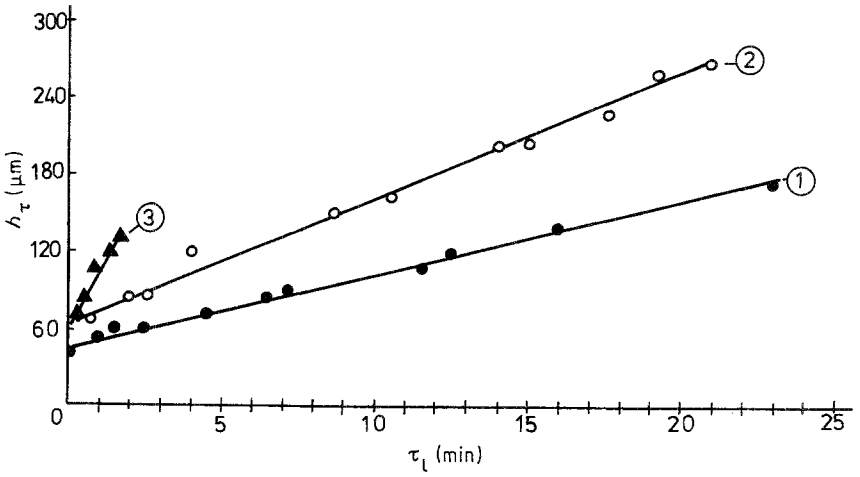

Fig. 7. Time dependence of the height, h_τ, of the hydrogen bubble during its attachment time in the range of the induction period.

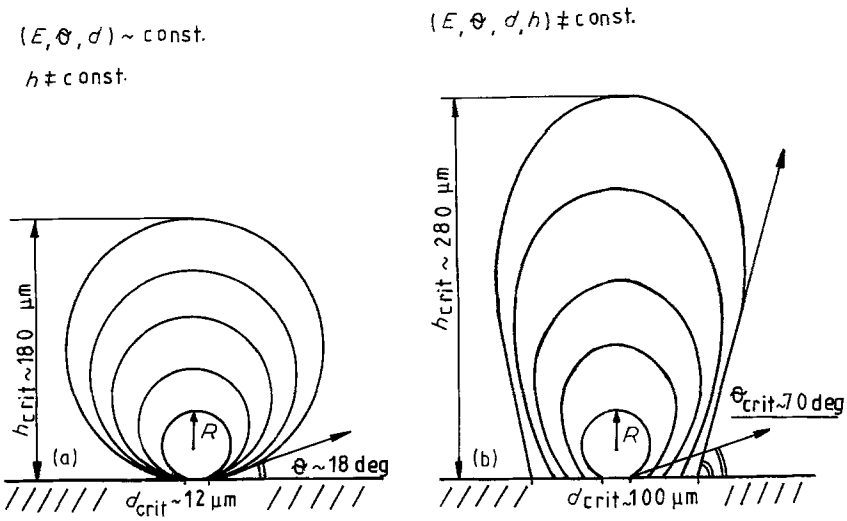

Fig. 8. Schematic representation of the growth of the hydrogen bubbles established in: (a) basic electrolyte or in electrolyte containing inhibitor and (b) basic electrolyte containing 10 mg l^{-1} Ni^{2+}.

of the hydrogen bubble shape from spherical at the beginning of the induction period to cupola-shaped at the end of it (Fig. 8b).

A logical conclusion is that the cathode surface, thus screened by the bubble (Fig. 9b), is no longer in electrical contact with the electrolyte, so the cathodic protection is lost. Under these conditions the screened zinc under the hydrogen bubble reaches a corrosion potential. On the other hand, reference data show [8] that the zero charge potential of zinc ($E_{zc} \sim -1.40\,V_{sse}$) in sulphuric acid is approximately equal to its corrosion potential in these electrolytes ($E_{cor} \sim -1.40\,V_{sse}$).

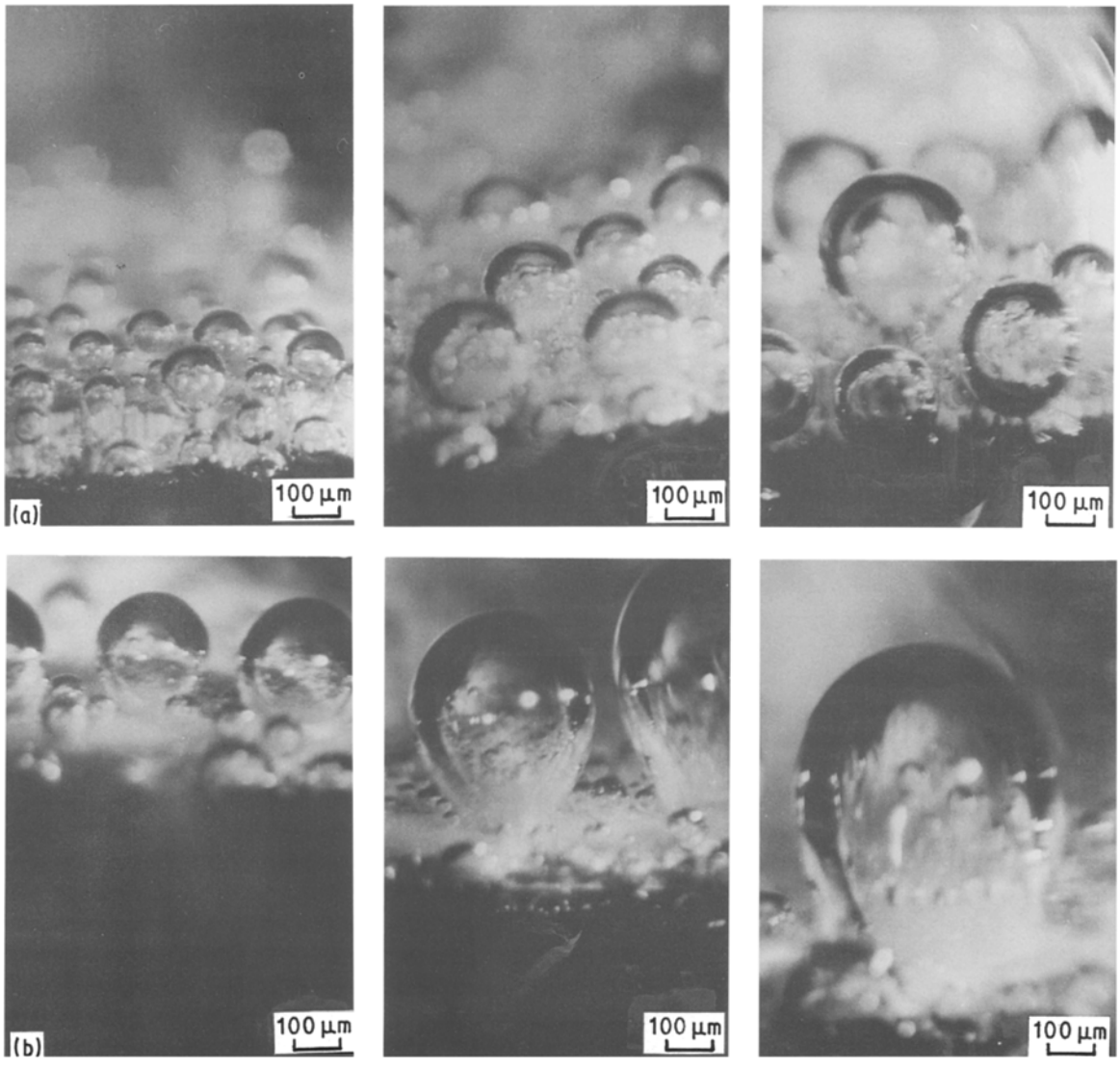

Fig. 9. Photographs of hydrogen bubbles formed during 1 h deposition time in: (a) basic electrolyte, T = 15–30–60 min and (b) basic electrolyte containing 10 mg l^{-1} Ni^{2+}, T = 15–30–60 min.

This enhances the formation of hydrogen bubbles with a maximum wetting angle (see Equations 2 and 5) or with maximum screening effect (Figs 8b and 9b). This is a prerequisite for the start of the active dissolution of the deposited zinc under bubbles [1].

Thus, the effect of the surfactant (inhibitor) can be explained by the strongly accelerated rate of hydrogen bubble growth (see Fig. 7, curve 3). Thus, hydrogen bubbles grow up to their critical sizes 7–8 times faster, reducing their attachment time. As a result their local screening effect is completely eliminated and, as seen in Fig. 2b, the surface is void of pitting defects.

5. Conclusion

Detailed polarization, volumetric and optical investigations of the hydrogen evolution rate during the electrowinning of zinc in the presence of a metal additive (Ni^{2+}) and organic inhibitors have confirmed the previously proposed [1] physical model for the nature of the induction period. It is shown that a characteristic feature of hydrogen bubbles growing on the electrode surface during the induction period is the pronounced increase of their wetting angle, θ, which results in a 10–12-fold larger diameter of the circle of the contact area with the cathode. As a result of the altered shape of the hydrogen bubbles from spherical at the beginning of the induction period to cupola-shaped at the end, the screening effect upon the cathode is also increased by an order of magnitude, thus allowing the zinc under the bubbles to reach its corrosion potential. Under these conditions, in the absence of cathodic protection, nickel codeposited with zinc forms a galvanic pair zinc–nickel with emf approximately 0.5 V, which explains the corrosion pits under the hydrogen bubbles.

Acknowledgements

The authors are grateful both to Dr. R. Wiart and to Dr. Fr. Huet (LP-15 du CNRS, France) for valuable discussions on the experimental results throughout this work.

References

[1] R. Wiart, C. Cachet, C. Bozhkov and St. Rashkov, *J. Appl. Electrochem.* **20** (1990) 381.
[2] D. Mackinnon, R. Morrison and J. Brannen, *ibid.* **16** (1986) 53.
[3] A. Frumkin, in 'Electrochemical Processes', Nauka Press, Moscow (1987) p. 171.
[4] B. Kabanov and A. Frumkin, *J. Phys. Chem., USSR*, **4** (1933) 538, 165, 433.
[5] A. Frumkin, A. Gorodezkaya, B. Kabanov and N. Nekrasov, *ibid.* **3** (1932) 351; **4** (1933) 529.
[6] R. Johnson and R. Dettre, in 'Wettability and Contact Angles – Surface and Colloid Science' (edited by E. Matijevic and F. Eirich), Wiley-Interscience, New York (1969) p. 85.
[7] *GIT Fachzeitschr. Laboratorium* **24** (1980) 642, 743, GIT Verlag Ernst Giebeler, Darmstadt.
[8] D. Dobos, 'Electrochemical Data', Mir Press, Moscow (1980) p. 249.